



Supplement of

Sulfate formation via aerosol-phase SO₂ oxidation by model biomass burning photosensitizers: 3,4-dimethoxybenzaldehyde, vanillin and syringaldehyde using single-particle mixing-state analysis

Liyuan Zhou et al.

Correspondence to: Liyuan Zhou (liyuanzhou3-c@my.cityu.edu.hk) and Chak K. Chan (chak.chan@kaust.edu.sa, chak.k.chan@cityu.edu.hk)

The copyright of individual parts of the supplement might differ from the article licence.

Text S1. Measurement of the photon flux.

In this work, 2-nitrobenzaldehyde (2NB), a chemical actinometer, was used to determine the photon flux in the OFR according to Liang et al. (2022). Briefly, a quartz glass vial containing 50 μM 2NB water solution was hung in the center of the OFR, and its photolysis was monitored by determining the concentration of 2NB every 5 min for a total of 25 min. The concentration of 2NB was measured using UHPLC-PDA (UHPLC, Waters Acquity H-Class, Waters, Milford, USA) and detailed settings can be found elsewhere (Mabato et al., 2022). The channel with UV absorption at 254 nm was used for the quantification of 2NB. The concentration of 2NB in the glass vial followed exponential decay, and its decay rate constant was determined using the following equation:

$$\ln\left(\frac{[2NB]_t}{[2NB]_0}\right) = -j(2NB) \times t, \quad (1)$$

where $[2NB]_t$ and $[2NB]_0$ are the 2NB concentrations at time t and 0, respectively. The following equation can also be used to calculate $j(2NB)$:

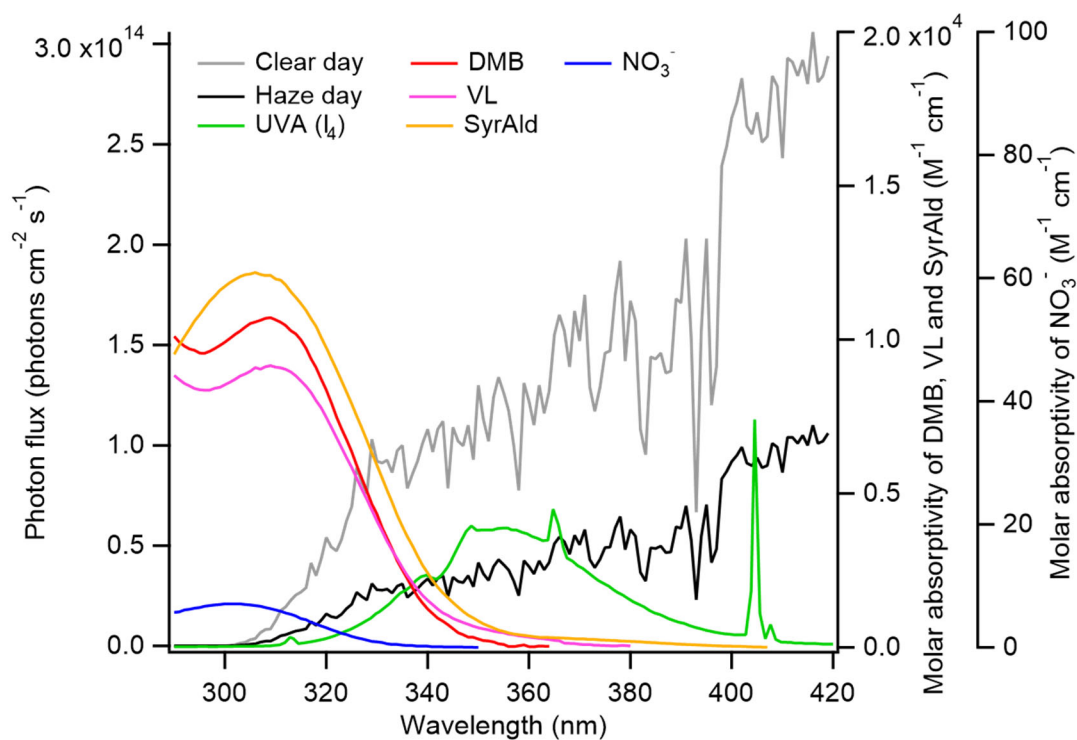
$$j(2NB) = 2.303 \times (10^3 \text{ cm}^3 \text{ L}^{-1} \times 1 \text{ mol/N}_A) \times \sum (I_\lambda \times \Delta\lambda \times \varepsilon_{2NB,\lambda} \times \Phi_{2NB}), \quad (2)$$

where N_A is Avogadro's number, I_λ is the actinic flux ($\text{photons cm}^{-2} \text{ s}^{-1} \text{ nm}^{-1}$), $\Delta\lambda$ is the wavelength interval between actinic flux data points (nm), and $\varepsilon_{2NB,\lambda}$ and Φ_{2NB} are the base-10 molar absorptivity ($\text{M}^{-1} \text{ cm}^{-1}$) and quantum yield ($\text{molecule photon}^{-1}$) for 2NB, respectively. Values of $\varepsilon_{2NB,\lambda}$ at each wavelength under 298 K and a wavelength-independent Φ_{2NB} were adapted from Galbavy et al. (2010). The transmission (%) of the quartz glass vial (one wall) was measured stable at $90 \pm 2\%$ (Liang et al., 2022), and therefore the photon flux was corrected by a factor of 1.11.

The spectral shape of the photon output of our illumination system (i.e., the relative flux at each wavelength) was measured using a high-sensitivity spectrophotometer (Brolight Technology Co. Ltd, Hangzhou, China). Using a scaling factor (SF), this measured relative photon output, $I_{\lambda, \text{relative}}$, is related to I_λ as follows:

$$I_\lambda = I_{\lambda, \text{relative}} \times \text{SF}, \quad (3)$$

I_λ was obtained by combining (1), (2), and (3), as shown in Figure S1. The actinic flux during typical haze over Beijing (40°N , 116°E) on January 26, 2015 at 12:00 pm (GMT+8) was estimated using the National Center for Atmospheric Research Tropospheric Ultraviolet Visible (TUV) Radiation Model (Figure S1) (Che et al., 2015; Che et al., 2014). The input environmental parameters were set to be as follows: clouds optical depth = 0, base = 4, top = 5; aerosol optical depth = 2.3, single scattering albedo = 0.9, Angstrom exponent = 0.9; direct beam = diffuse down = diffuse up = 1. For clear days, the actinic flux was estimated over Beijing (at the same date and time) using the default parameters.



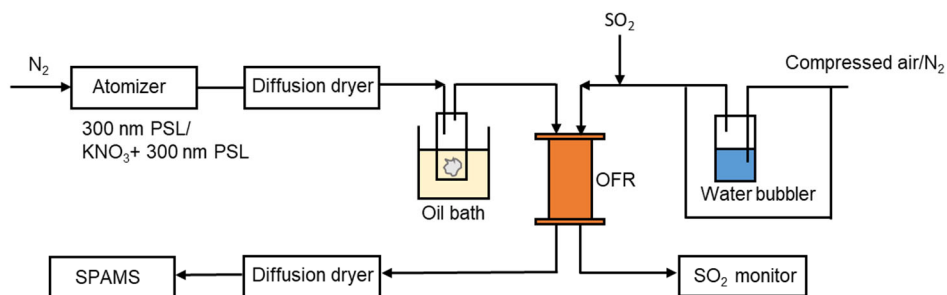
39

40 **Figure S1.** The molar absorptivities (ϵ , $M^{-1} cm^{-1}$) of DMB, VL, SyrAld and NO_3^- , and photon flux in the OFR (I_4) and during

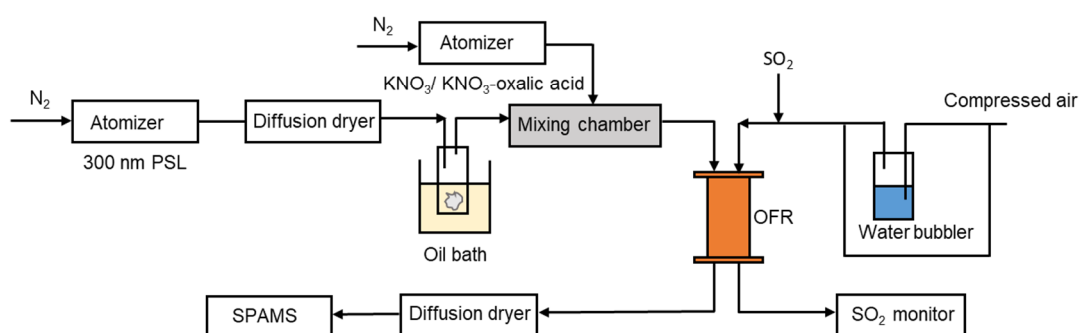
41 typical haze days or clear days in Beijing, China.

42

(a)



(b)



44

45

Figure S2. Schematic of the experimental setups for the generation of (a) DMB-, VL-, SyrAld-, or BA-coated particles and

46

internally mixed particles of KNO_3 and VL and (b) externally mixed aerosol composed of a mix of KNO_3 and VL-coated

47

particles. The coated particles were sent to the OFR for SO_2 exposure and analyzed by the SPAMS for size and composition.

48

49

50

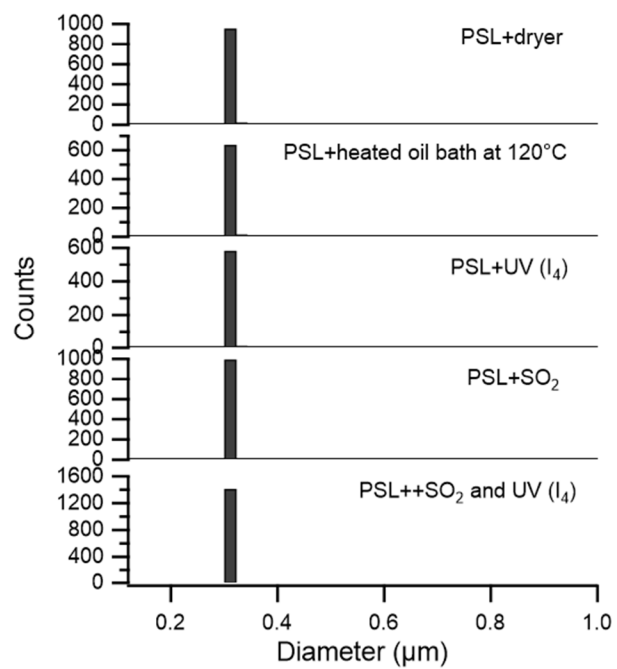
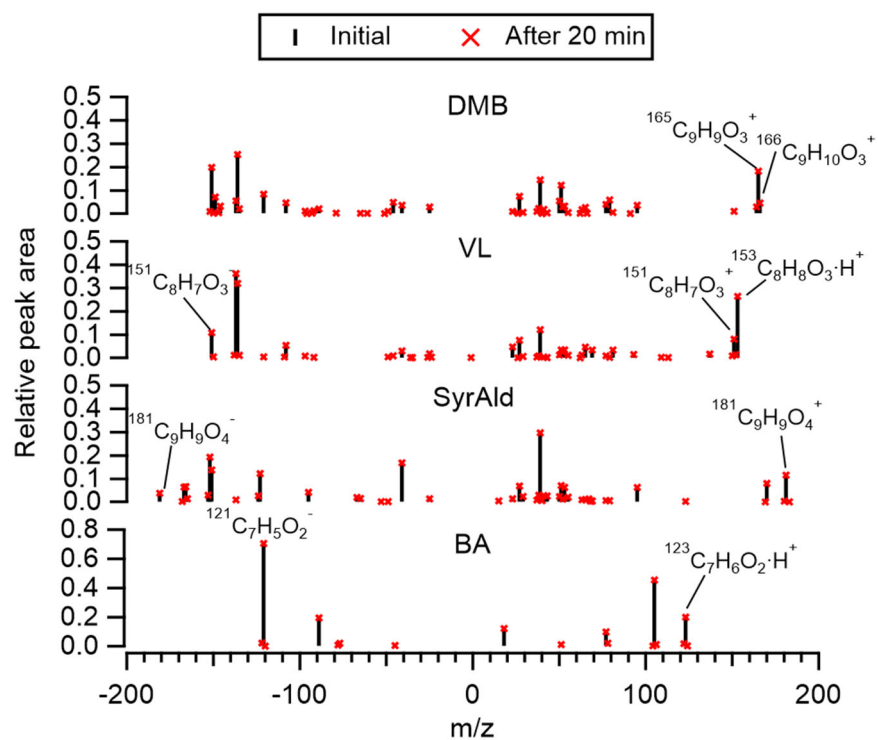


Figure S3. PSL condensation nuclei size characterization using SPAMS.



55

56 **Figure S4.** Mass spectra of the DMB-, VL-, SyrAld- and BA-coated particles at the beginning of the experiments (initial) and57 the end of the experiments (after 20 min) in the absence of light and SO_2 .

58

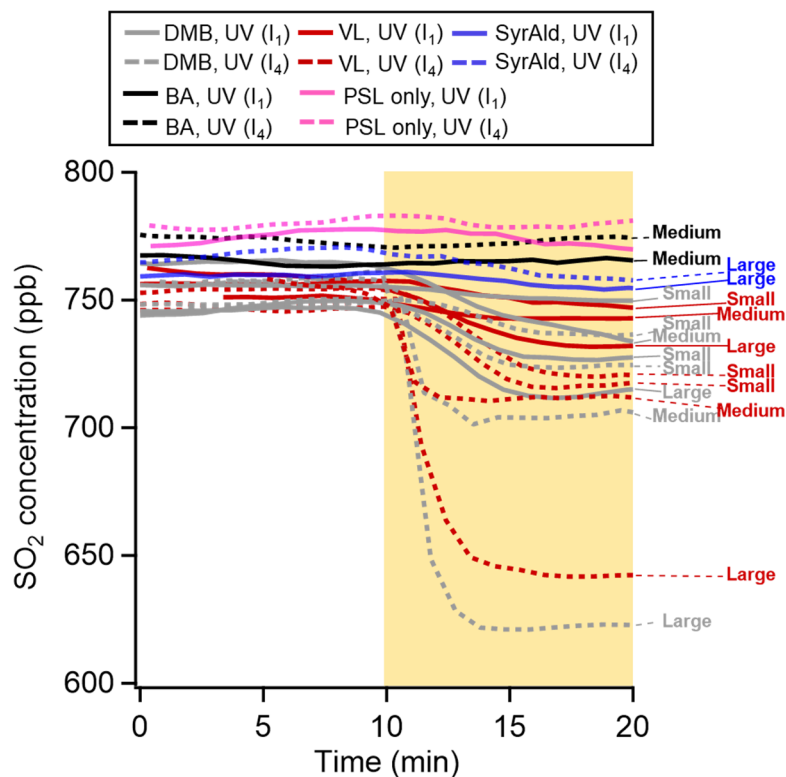


Figure S5. Time traces of SO₂ in the dark (0-10 min) and under UV irradiation (I₁ and I₄) (10-20 min) in the presence of DMB-, VL-, SyrAld-, or BA-coated particles and PSL-only particles. The SO₂ consumption is presented as a function of the total surface area concentration of SPAMS detected particles. Total surface area concentrations in the range of 7×10^4 - 2×10^5 μm^2 m^{-3} are denoted by “small”, in 2×10^5 - 6×10^5 μm^2 m^{-3} as “medium”, and larger than 6×10^5 μm^2 m^{-3} as “large”.

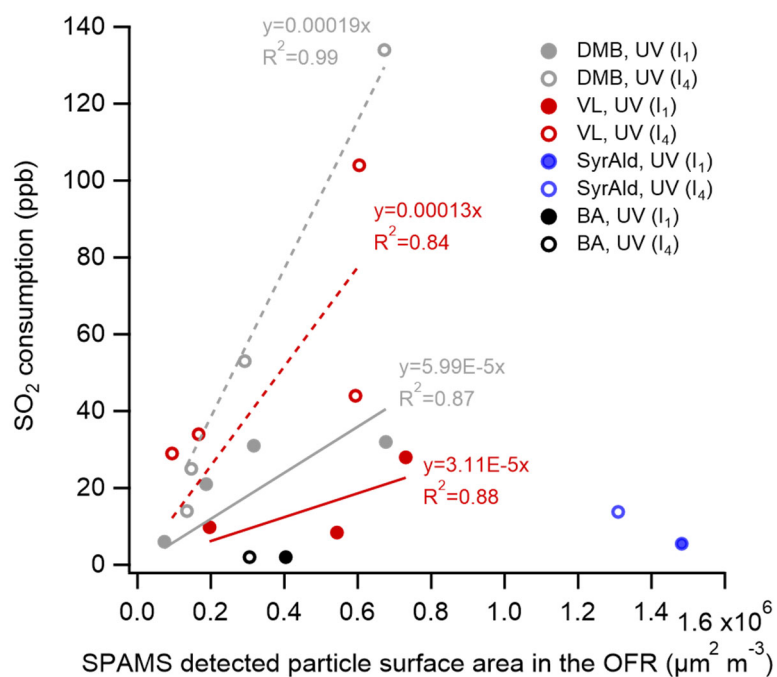


Figure S6. The SO₂ consumption under UV irradiation vs. the surface area of SPAMS detected particles in the OFR for DMB-, VL-, SyrAld- and BA-coated particles under UV irradiation and SO₂.

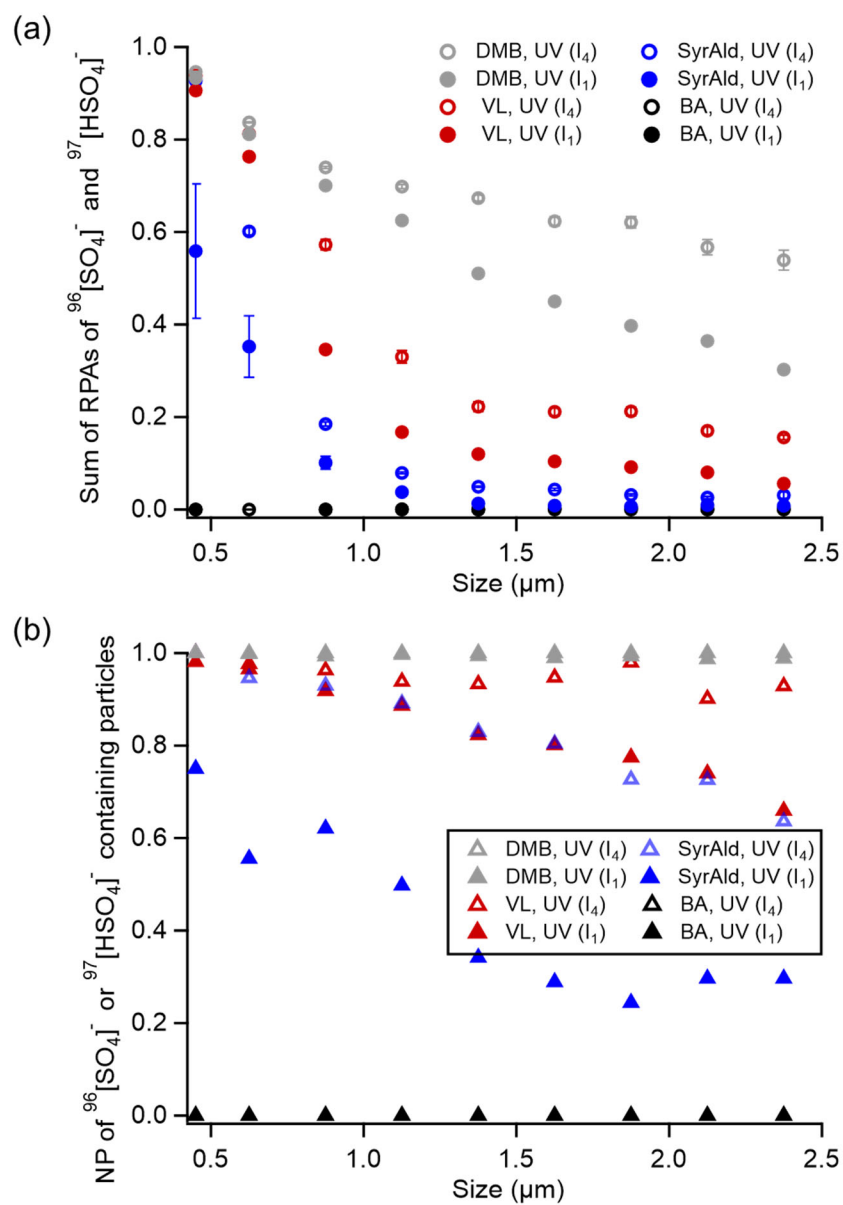


Figure S7. Size-dependent (a) RPA and (b) number percentage (NP) of sulfate for DMB-, VL-, SyrAld- and BA-coated particles under UV irradiation and in the presence of SO_2 . Errors are shown by 95% confidence intervals.

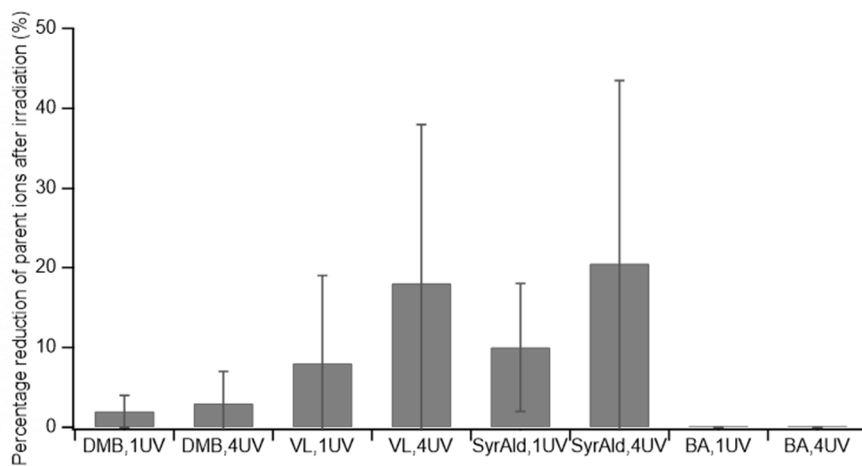


Figure S8. The percentage reduction of the RPA of parent ions in the positive spectra after UV irradiation. Error bars represent the standard deviation (1σ).

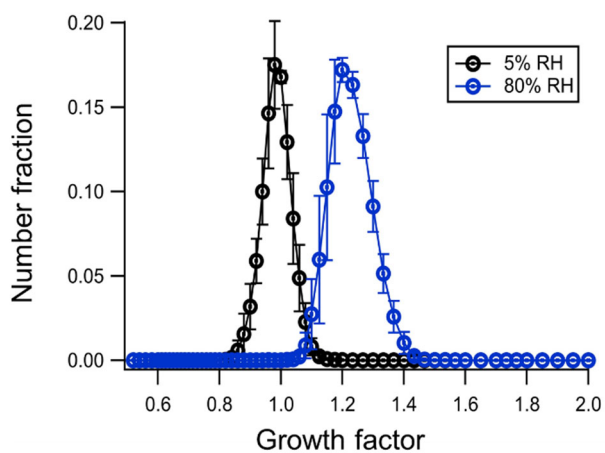


Figure S9. Hygroscopic growth factor distribution for KNO_3 particles at 5% and 80% RH. The measurements were performed using a Hygroscopicity-tandem differential mobility analyzer (HTDMA) system (Model 3100, Brechtel Manufacturing Inc, USA). Error bars represent the standard deviation (1σ).

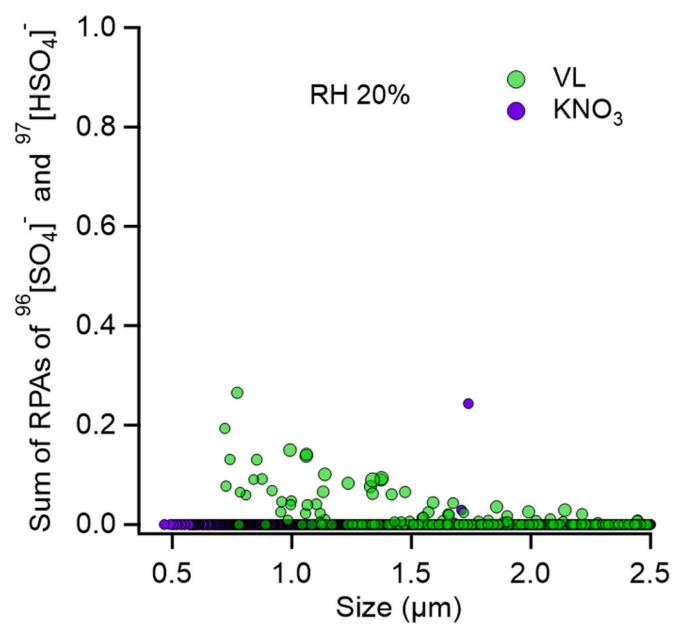


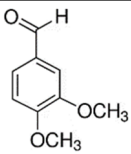
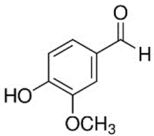
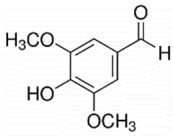
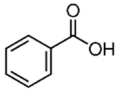
Figure S10. Sulfate RPA vs. particle diameter detected by the SPAMS for externally mixed VL-coated particles and KNO_3 at 20% RH under UV irradiation (I_1) in the presence of SO_2 .

Reaction conditions	RH (%)	Gas in the OFR	UV intensity (photon cm ⁻² s ⁻¹)
DMB-coated particles	80	CA ^a and N ₂	I ₁ and I ₄ ^b
VL-coated particles	80	CA ^a and N ₂	I ₁ and I ₄ ^b
SyrAld-coated particles	80	CA ^a and N ₂	I ₁ and I ₄ ^b
BA-coated particles	80	CA ^a	I ₁ and I ₄ ^b
Externally mixed VL-coated particles and KNO ₃	80 and 20	CA ^a	I ₁ ^b
Externally mixed VL-coated particles and KNO ₃ -oxalic acid particles	80	CA ^a	I ₁ ^b
Internally mixed VL and KNO ₃ particles	80	CA ^a	I ₁ ^b

^a HEPA-filtered and activated-carbon-denuded compressed air.

^b One and four lamps to provide a total irradiance of about 1.1×10^{15} (I₁) and 3.8×10^{15} (I₄) photon cm⁻² s⁻¹, respectively.

Table S2. Chemical formula, structure, molar mass and property of the chemicals used in this study.

Chemical compound	Formula	Structure	Molar mass (g mol ⁻¹)	Property ^a
3,4-dimethoxybenzaldehyde	C ₉ H ₁₀ O ₃		166.17	non-phenolic methoxybenzaldehyde photosensitizer
vanillin	C ₈ H ₈ O ₃		152.15	phenolic methoxybenzaldehyde photosensitizer
syringaldehyde	C ₉ H ₁₀ O ₄		182.17	phenolic methoxybenzaldehyde photosensitizer
benzoic acid	C ₇ H ₆ O ₂		122.123	non- photosensitizer

^aThe Photosensitizing properties are derived from the literature (Smith et al., 2015, 2016; Smith et al., 2014).

100 REFERENCES

- 101 Che, H., Xia, X., Zhu, J., Li, Z., Dubovik, O., Holben, B., Goloub, P., Chen, H., Estelles, V., and Cuevas-Agulló, E.: Column
 102 aerosol optical properties and aerosol radiative forcing during a serious haze-fog month over North China Plain in 2013 based
 103 on ground-based sunphotometer measurements, *Atmospheric Chemistry and Physics*, 14, 2125-2138, 2014.
- 104 Che, H., Xia, X., Zhu, J., Wang, H., Wang, Y., Sun, J., Zhang, X., and Shi, G.: Aerosol optical properties under the condition
 105 of heavy haze over an urban site of Beijing, China, *Environmental Science and Pollution Research*, 22, 1043-1053, 2015.
- 106 Galbavy, E. S., Ram, K., and Anastasio, C.: 2-Nitrobenzaldehyde as a chemical actinometer for solution and ice photochemistry,
 107 *Journal of Photochemistry and Photobiology A: Chemistry*, 209, 186-192, 2010.
- 108 Liang, Z., Zhou, L., Infante Cuevas, R. A., Li, X., Cheng, C., Li, M., Tang, R., Zhang, R., Lee, P. K., and Lai, A. C.: Sulfate
 109 Formation in Incense Burning Particles: A Single-Particle Mass Spectrometric Study, *Environmental Science & Technology*
 110 *Letters*, 2022.
- 111 Mabato, B. R. G., Lyu, Y., Ji, Y., Li, Y. J., Huang, D. D., Li, X., Nah, T., Lam, C. H., and Chan, C. K.: Aqueous secondary
 112 organic aerosol formation from the direct photosensitized oxidation of vanillin in the absence and presence of ammonium
 113 nitrate, *Atmospheric Chemistry and Physics*, 22, 273-293, 2022.
- 114 Smith, J. D., Sio, V., Yu, L., Zhang, Q., and Anastasio, C.: Secondary organic aerosol production from aqueous reactions of
 115 atmospheric phenols with an organic triplet excited state, *Environmental science & technology*, 48, 1049-1057, 2014.
- 116 Smith, J. D., Kinney, H., and Anastasio, C.: Aqueous benzene-diols react with an organic triplet excited state and hydroxyl
 117 radical to form secondary organic aerosol, *Physical Chemistry Chemical Physics*, 17, 10227-10237, 2015.
- 118 Smith, J. D., Kinney, H., and Anastasio, C.: Phenolic carbonyls undergo rapid aqueous photodegradation to form low-volatility,
 119 light-absorbing products, *Atmospheric Environment*, 126, 36-44, 2016.

120